

Silaindacenodithiophene Semiconducting Polymers for Efficient Solar Cells and High-Mobility Ambipolar Transistors[†]

Raja Shahid Ashraf,^{*,‡} Zhuoying Chen,^{*,§}
Dong Seok Leem,[‡] Hugo Bronstein,[‡] Weimin Zhang,^{‡,||}
Bob Schroeder,[#] Yves Geerts,[#] Jeremy Smith,[‡]
Scott Watkins,[‡] Thomas D. Anthopoulos,[‡]
Henning Sirringhaus,[§] John C. de Mello,[‡]
Martin Heeney,[‡] and Iain McCulloch[‡]

[‡]Imperial College, London SW72AZ, United Kingdom,

[§]Cavendish Laboratory, University of Cambridge,

J.J. Thompson Avenue, Cambridge CB3 0HE, United Kingdom,

[‡]CSIRO Molecular and Health Technologies, Victoria 3169,

Australia, ^{||}Guangxi University for Nationalities, Nanning

530006, P.R. China, and [#]Université Libre de Bruxelles

Received October 15, 2010

Revised Manuscript Received November 25, 2010

A novel fused coplanar chromophore, silaindacenodithiophene (SiIDT), as shown in Figure 1, is reported along with the synthesis and semiconducting properties of two SiIDT alternating copolymers in field-effect transistor and photovoltaic devices. Recently, we have shown that alternating copolymers of indacenodithiophene with both thieno[3,2-b]thiophene and benzothiadiazole exhibit very high hole mobility.¹ Further extending the design concept of this class of polymers to enhance both the electron mobility and photovoltaic properties, we have replaced the bridging carbons of the indacenodithiophene unit with silicon as well as also introduced as comonomers the electron-poor and highly polar 1,4-diketopyrrolo[3,4-c]pyrrole (DPP) unit, which has previously exhibited both ambipolarity² and more recently, good photovoltaic efficiencies.³ The longer silicon–carbon bond increases the separation between antibonding lobes of the coupled aryl units on the SiIDT, thus reducing the energy of the HOMO energy level. It had also been reported that the LUMO of silole conjugated polymers has additional stability arising from the in-phase mixing of σ^* and π^* orbitals from the silylene and conjugated moieties.⁴ This more stable LUMO would be expected to facilitate improved electron transport and stability, as well as reduce the bandgap, leading to enhanced photocharge generation.

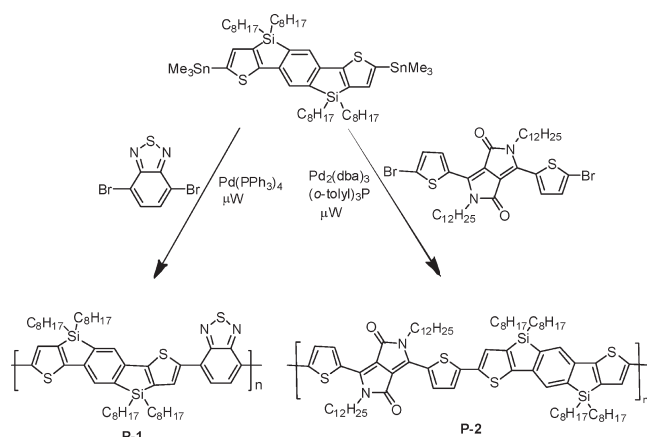


Figure 1. Polymerization and molecular structure of silaindacenodithiophene copolymers with benzothiadiazole (P-1) and DPP (P-2).

Two repeat units were selected for copolymerization. The electron poor benzothiadiazole unit facilitates molecular hybridization with the SiIDT unit, leading to low band-gaps, required for high-performing solar cell devices. The 1,4-diketopyrrolo[3,4-c]pyrrole (DPP), as a consequence of its synthesis, has peripheral unsubstituted thiophene units that can assist in backbone planarity, whereas the bis-amide units of the pyrrolopyrrole are electron-withdrawing, thus assisting molecular hybridization and thus a low band gap. The pyrrole functionality is strongly polar, which assists in intermolecular associations and improves charge transport, and the nitrogens are alkyl functionalized to promote solubility. Linear chains were required in this polymer system to ensure good charge transport.

Polymers P-1 and P-2 were both synthesized (see the Supporting Information) by Stille cross coupling, as shown in Figure 1, using microwave heating conditions.⁵ Polymerizations proceeded in good yield when the stannyl groups were located on the electron rich SiIDT, with sufficiently high molecular weights obtained (see Table 1). Both copolymers are soluble in common organic solvents such as THF, chloroform, toluene, and chlorobenzene. The thin-film optical absorption spectra of the polymers display long wavelength maxima (Table 1 and the Supporting Information). Both polymers show evidence of crystallinity when evaluated by differential scanning calorimetry (DSC) as shown in Supporting Information. Polymer P-1 exhibits a low enthalpy melting endotherm at about 325 °C, whereas P-2 has a more pronounced melt at about 300 °C. These high-temperature melts are consistent with the fused aromatic molecular motif of the polymer backbone.

By replacing the BT unit (P-1) with DPP (P-2), a red-shifted absorption spectrum with more defined vibronic

[†] Accepted as part of the “Special Issue on π -Functional Materials”.

^{*}Corresponding author. E-mail: r.ashraf@imperial.ac.uk (R.S.A.); zc234@cam.ac.uk (Z.C.).

- (1) Zhang, W.; Smith, J.; Watkins, S. E.; Gysel, R.; McGehee, M.; Salleo, A.; Kirkpatrick, J.; Ashraf, S.; Anthopoulos, T.; Heeney, M.; McCulloch, I. *J. Am. Chem. Soc.* **2010**, *132*, 11437–11439.
- (2) Bürgi, L.; Turbiez, M.; Pfeiffer, R.; Bienewald, F.; Kirner, H. J.; Winnewisser, C. *Adv. Mater.* **2008**, *20*, 2217–2224.
- (3) Bijleveld, J. C.; Gevaerts, V. S.; Di Nuzzo, D.; Turbiez, M.; Mathijssen, S. G. J.; de Leeuw, D. M.; Wienk, M. M.; Janssen, R. A. J. *Adv. Mater.* **2010**, *22*, 242–246.
- (4) Yamaguchi, S.; Tamao, K. *J. Chem. Soc., Dalton Trans.* **1998**, *0*, 3693–3702.

- (5) Tierney, S.; Heeney, M.; McCulloch, I. *Synth. Met.* **2005**, *148*, 195–198.

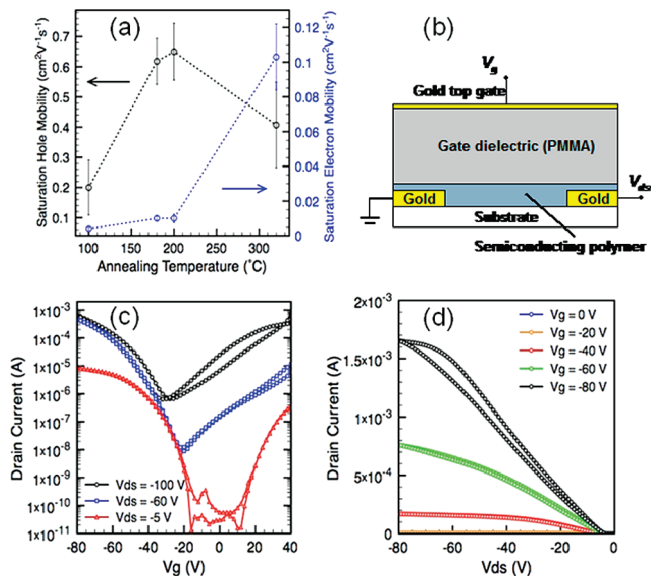


Figure 2. (a) Effect of annealing temperature on the saturation hole and electron mobility of P-2. 100 °C corresponds to as-spun conditions. Each data point was averaged on 6–7 devices ($L = 20 \mu\text{m}$, $W = 1$ or 2 cm) with error bars of one standard derivation. (b) Schematic of the bottom contact/top gate transistor structure. (c) Transfer characteristics of a P2 FET annealed at 320 °C under different bias conditions ($L = 20 \mu\text{m}$, $W = 1 \text{ cm}$) with $\mu_h \sim 0.32 \text{ cm}^2 \text{ V}^{-1} \text{ s}^{-1}$ and $\mu_e \sim 0.12 \text{ cm}^2 \text{ V}^{-1} \text{ s}^{-1}$. (d) Output characteristics of a P-2 FET annealed at 180 °C. All FETs shown in this figure were fabricated with $\sim 550 \text{ nm}$ thick PMMA as the gate dielectric (capacitance $C_i = 6.2 \text{ nF cm}^{-2}$).

Table 1. Properties of Copolymers

polymer	co-repeat unit	M_n/M_w (kg/mol)	λ_{max} (film) (nm)	μ_h/μ_e (max) ($\text{cm}^2 \text{ V}^{-1} \text{ s}^{-1}$)
P-1	BT	30/61	634	0.008/—
P-2	DPP	29/80	755	0.65/0.1

structure is obtained. This is indicative of a planarization of the conjugated backbone and a π stacked microstructure. From the onset of the absorption spectra, optical bandgap values of about 1.8 and 1.4 eV were estimated for polymers P-1 and P-2, respectively. The HOMO energy levels of both polymers were estimated by ambient photoelectron spectroscopy (PESA) (P-1, -5.5 eV ; P-2, -5.1 eV). The deep HOMO level ensures that the P-1 is stable against electrochemical oxidation, and thus good device life times can be expected. In addition, because V_{oc} is determined by the energy-level difference between the HOMO level of the donor and the LUMO level of the acceptor components,⁶ a deeper donor HOMO level blended with [70]PCBM results in a higher V_{oc} value, which is reflected in the J – V characteristics (Figure 3a).

Both as-spun and annealed P-2 FET devices (shown in Figure 2b) show clear ambipolar characteristics. As-spun hole and electron mobility extracted from the saturation regime of the transfer curve is ~ 0.2 and $\sim 0.004 \text{ cm}^2 \text{ V}^{-1} \text{ s}^{-1}$, respectively, where the ON–OFF ratio ($I_{\text{on}}/I_{\text{off}}$) is $\sim 1 \times 10^5$ to 1×10^6 for p-channel operation and $\sim 1 \times 10^3$ for n-channel operation. Significant improvement of

Table 2. Properties of Copolymers

polymer	HOMO (eV)	LUMO (eV)	V_{oc} (V)	J_{sc} (mA/cm ²)	FF	PCE (%)
P-1	−5.5	−3.6	0.88	9.39	0.52	4.3
P-2	−5.1	−3.7	0.63	3.53	0.65	1.4

device performance was observed upon annealing at temperatures slightly higher than the melt, prior to gate dielectric deposition. In particular, when the polymer films were annealed at 320 °C, the electron mobility significantly increases to $\sim 0.1 \text{ cm}^2 \text{ V}^{-1} \text{ s}^{-1}$ with $\sim 1 \times 10^5$ in $I_{\text{on}}/I_{\text{off}}$. This leads to balanced and efficient ambipolar transport as the hole mobility drops to ~ 0.4 with $\sim 1 \times 10^5$ to 1×10^6 in $I_{\text{on}}/I_{\text{off}}$. Mobility values of P-2 FETs using different annealing temperatures are plotted in Figure 2a and typical transfer and output FET characteristics are shown in panels c and d in Figure 2.

Although the hole mobilities maximize at a lower temperature than the melt (approximately 200 °C), an order of magnitude increase in electron mobility was obtained upon annealing above the phase transition. Such an increase in electron mobility may arise from polymer reorganization after phase transition resulting in a microstructure more favorable for electron transport. In donor–acceptor type polymer, F8BT, electron transport has been suggested to mainly rely on the efficiency in interchain hopping and thus sensitive to the relative registration of BT units between adjacent polymer chains. P-2 is also a donor–acceptor type polymer and its electron transport is expected to be sensitive to the local microstructure, in particular the interchain distances between electron-withdrawing DPP units where the LUMO is localized.⁷ UV–vis absorptions of P-2 films from as-spun condition and annealed above its melting temperature show different vibronic structure in its absorption band, indicating different intermolecular aggregations (see the Supporting Information). Electron transport has been previously suggested to be sensitive to extrinsic electronegative impurities such as hydroxyl groups (moisture) and oxygen.^{8,9} Tiny amount of impurities can exist in the semiconducting polymer and/or the solvent from synthetic residues or the fabrication process. Annealing the polymer films above its melting point under nitrogen may help to remove physically or chemically attached impurities and residue solvent and thus improves electron mobility.

The photovoltaic properties of P-1 and P-2 were investigated in the device structure ITO/PEDOT:PSS/P-1:[70]PCBM/Ca or LiF/Al (see the Supporting Information) and the details reported in Table 2. The electron acceptor [70]PCBM was chosen, as its short wavelength absorption is complementary to the polymer absorption.¹⁰

(6) Brabec, C. J.; Cravino, A.; Meissner, D.; Sariciftci, N. S.; Fromherz, T.; Rispens, M. T.; Sanchez, L.; Hummelen, J. C. *Adv. Funct. Mater.* **2001**, *11*, 374–380.

(7) Donley, C. L.; Zaumseil, J.; Andreasen, J. W.; Nielsen, M. M.; Sirringhaus, H.; Friend, R. H.; Kim, J.-S. *J. Am. Chem. Soc.* **2005**, *127*, 12890–12899.
(8) Chua, L. L.; Zaumseil, J.; Chang, J. F.; Ou, E. C. W.; Ho, P. K. H.; Sirringhaus, H.; Friend, R. H. *Nature* **2005**, *434*, 194–199.
(9) Sirringhaus, H. *Adv. Mater.* **2009**, *21*, 3859–3873.
(10) Wienk, M. M.; Kroon, J. M.; Verhees, W. J. H.; Knol, J.; Hummelen, J. C.; van Hal, P. A.; Janssen, R. A. J. *Angew. Chem., Int. Ed.* **2003**, *42*, 3371–3375.

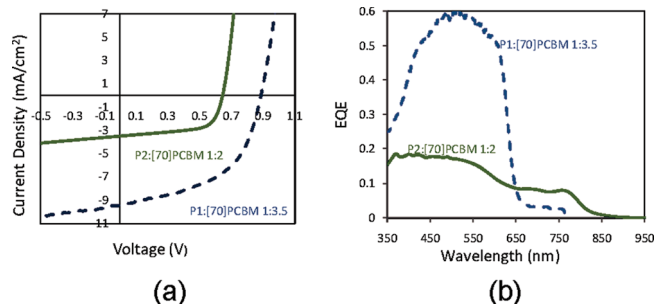


Figure 3. (a) I – V characteristics of a P-1/P2:[70]PCBM solar cell under AM1.5 solar illumination and (b) external quantum efficiencies of the cells.

The high optimal ratio of fullerene, particularly in the P-1 devices, indicates that it is likely that the fullerene has a high incorporation within the polymers.¹¹ The low lying HOMO energy level of P-1 promotes the larger V_{oc} exhibited by the P-1 devices, shown in Figure 3a, and with the low bandgap also contributing to good current density, a relatively large PCE was obtained.

The photocurrent of solar cells at optimized conditions under monochromatic illumination was recorded, and a

mismatch factor was calculated at AM1.5 light intensity. The external quantum efficiency (EQE) of both polymer solar cells are shown in Figure 3b. It is clear that the photocurrent in both devices is generated from the photo-excitation states in both the polymer and [70]PCBM. The complementary absorbance of P-1 and [70]PCBM contribute to an EQE of over 40% from 400 to 640 nm wavelengths with an onset at 710 nm. This broad coverage of the solar spectrum generates a good J_{sc} under illumination. In contrast, the EQE of P-2, reached only up to 15%, which we attribute to the lower LUMO–LUMO offset energy between P2 and [70]PCBM, which may be less than necessary for efficient electron transfer.^{12,13,14} This low EQE correlates with the low currents obtained from P-2 devices. Both polymer systems are currently far from optimized, and in particular, optimization of silaindacenodithiophene side chain length and branching would be expected to further increase device performance.

New silaindacenodithiophene semiconducting polymers have been reported. These polymers can exhibit either high solar cell efficiencies of greater than 4% PCE, or high ambipolar charge transport, with holes and electrons exhibiting mobilities of greater than 0.1 cm²/(V s).

Acknowledgment. This work was in part carried out under the EC FP7 ONE-P Project 212311 and DPI Grant 678.

Supporting Information Available: Synthesis of monomers and copolymers, UV–vis absorption spectra, DSC traces, transistor characteristics. This material is available free of charge via the Internet at <http://pubs.acs.org>

- (11) Mayer, A. C.; Toney, M. F.; Scully, S. R.; Rivnay, J.; Brabec, C. J.; Scharber, M.; Koppe, M.; Heeney, M.; McCulloch, I.; McGehee, M. D. *Adv. Funct. Mater.* **2009**, *19*, 1173–1179.
- (12) Halls, J. J. M.; Cornil, J.; dos Santos, D. A.; Silbey, R.; Hwang, D. H.; Holmes, A. B.; Bredas, J. L.; Friend, R. H. *Phys. Rev. B* **1999**, *60*, 5721.
- (13) Veldman, D.; Bastiaansen, J. J. A. M.; Langeveld-Voss, B. M. W.; Sweelssen, J.; Koetse, M. M.; Meskers, S. C. J.; Janssen, R. A. J. *Thin Solid Films* **2006**, *511–512*, 581–586.
- (14) Ohkita, H.; Cook, S.; Astuti, Y.; Duffy, W.; Tierney, S.; Zhang, W.; Heeney, M.; McCulloch, I.; Nelson, J.; Bradley, D. D. C.; Durrant, J. R. *J. Am. Chem. Soc.* **2008**, *130*, 3030–3042.